Journal of Hydrology 528 (2015) 694–702

Contents lists available at ScienceDirect

Journal of Hydrology

journal homepage: www.elsevier.com/locate/jhydrol

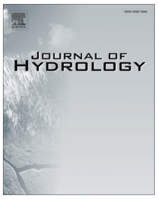

Experimental evidence of how the fractal structure controls the hydrodynamic resistance on granular aggregates moving through water

Federico Maggi

School of Civil Engineering, The University of Sydney, Bld. J05, 2006 Sydney, NSW, Australia

ARTICLE INFO

Article history:
Received 14 October 2014
Received in revised form 1 May 2015
Accepted 3 July 2015
Available online 9 July 2015
This manuscript was handled by Laurent Charlet, Editor-in-Chief, with the assistance of Nicolas Gratiot, Associate Editor

Keywords:
Fractal
Aggregate
Drag
Inertia
Experiment
3D printing

SUMMARY

A comprehensive set of experiments was carried out to investigate the effect of the fractal architecture of granular aggregates on the free-fall acceleration through a still water column. Test aggregates were first generated numerically with a method that allowed to control the fractal dimension d and, next, three stochastic replicates were lithographically fabricated for each of six values of d ranging between 1.9 and 2.7. The recorded position, velocity and acceleration served to analyze their dynamics in the Reynolds and Galilei number space, and to calculate the momentum rate of change and the intensity of drag (viscous and impact) and inertial forces (added mass and Basset–Bousinnesq). Analysis of these forces highlighted a strong dependence on d; additionally, integration of these forces in the particle momentum equation allowed to identify an additional resistance R_x that showed a strong correlation with d. A correlation analysis of R_x with various scaling laws combining velocity and acceleration suggested that R_x could be described by a nonlinear drag force and a force intermediate between drag and inertia. It was therefore concluded that irregular granular fractal aggregates accelerating in water are subject to highly complex and nonlinear hydrodynamic effects caused by surface roughness and volume porosity, and that these effects have tight connection with the internal and external fractal characteristics of the aggregates.

1. Introduction

The way suspended particles and aggregates move through water has been under the attention of many disciplines related to environmental flows, but is of particular interest in the sediment dynamics area because of the large scale repercussions advected and deposited sediment have on hydrological and morphodynamic processes (Dyer, 1989; Seminara and Blodeaux, 2001; McAnally and Mehta, 2001) as well as water quality and ecosystem stability in reservoirs, rivers, estuaries, coastal and marine ecosystems (Picouet et al., 2001; Cloern, 2001; Thornton, 2002; Stemmann et al., 2004; Kiorboe, 2001; Maggi, 2009).

Cohesive mineral and organic particulate present in aqueous environments is normally subject to processes of aggregation that change the aggregate size distribution and greatly affect the fraction of suspended matter that is subject to advection or deposition. Aggregates formed in aqueous environments normally have fractal architectures as they result from a statistically self-similar assemblage of lower-order aggregates (Meakin, 1991; Vicsek, 1992; Kranenburg, 1994). In general, aggregation lowers the fractal dimension d of resulting aggregates as compared to the forming ones, while breakup increases it (Maggi, 2007). Changes in fractal dimension also depend on the source matter (e.g., mineral and organic), biological presence (e.g., cell colonization), environmental conditions (e.g., shear rate, chemistry, etc.), and on whether aggregates deform when moving. The aggregate hydrodynamics may substantially be affected by its geometrical characteristics and, in particular, its fractal dimension, which can be used to scale various geometrical properties (e.g., volume, surface, size, porosity, etc., Kranenburg, 1994) and physical properties (e.g., density, settling velocity, stiffness, etc., Winterwerp, 1999; Maggi, 2007) as well as particle–particle interaction kinematics and reaction rates (e.g., collision, deformation, aggregation, breakup, Maggi et al., 2007). For example, compact and dense granular aggregates (e.g., small aggregates of cohesive minerals) may show dynamical features and move through water relatively similarly to solid particles of the same size (e.g., small silt grains); conversely, chain-like, fluffy organic aggregates that show clusters of masses attached by biological filaments (e.g., large organic aggregates, marine snow, Alldredge and Gotschalk, 1989) have been shown to move through

---

E-mail address: federico.maggi@sydney.edu.au

http://dx.doi.org/10.1016/j.jhydrol.2015.07.002
0022-1694/© 2015 Elsevier B.V. All rights reserved.

water with substantially lower velocity as compared to particles of equivalent size (e.g. Vahedi and Gorczyca, 2012; Maggi, 2013).

A number of works have highlighted that the hydrodynamics of solid smooth spheres (e.g., Clift and Gauvin, 1971; Blevins, 1984; Brown and Lawler, 2003) strongly differs from that of solid sphere with rough surface (experiments in Achenbach, 1974), spheres with porous coating (numerically in Taamneh and Bataineh, 2011), porous spheres (numerically in Joseph and Tao, 1964; Jain and Basu, 2012), and various other shapes (Blevins, 1984; Chhabra et al., 1999). It is also well understood that irregular sand and silt particles are subject to higher drag (resistance) as compared to spherical solid particles of equivalent size (Rubey, 1933; Dietrich, 1982; Loth, 2008), and that drag is higher also for flocculated suspended particle matter (Hallermeier, 1981; Ahrens, 2000) presumably because of the complex geometry of surface asperities and pores. More recently, attempts have been undertaken to estimate the drag on fractal aggregates based on models of their internal geometry (Rogak and Flagan, 1990; Tang and Raper, 2002; Garcia-Ybarra et al., 2006) or by analysis of experimental data (Strom and Keyvani, 2011; Maggi, 2013).

A large consensus emerges from the above works on the fact that irregularities at the surface as well as the presence of (open) pores generally increase the drag (up to about 6 times, Strom and Keyvani, 2011) over a relatively wide range of Reynolds numbers $Re = \rho_w L v/\mu$, with ρ_w and μ the water specific density and viscosity, respectively, and L and v the characteristic length scale and velocity of the aggregate. If these notions are now relatively well consolidated for stationary conditions, that is, when motion is uniform, less knowledge is currently available on the contributions to resistance when the motion is non-uniform, that is, when aggregates undergo an acceleration due to the gravitational force or other. In this case, not only drag but also inertial forces act on the aggregates; for granular fractal aggregates, both drag and inertial forces may be associated to the fractal dimension as this can be used to scale the capacity of pores and the solid skeleton, as well as surface roughness; however, a detailed analysis with control test specimens is currently not available to the best of the author's knowledge.

The aim of this paper is to provide experimental evidence that the intensity of (drag and inertia) resistance to the accelerated motion of granular aggregates depends on the fractal dimension of their architecture. This evidence was substantiated by the experimental procedure, which allowed to fabricate aggregates with arbitrary fractal dimension. Experimentally observed kinematic and dynamic quantities of free-falling granular fractal aggregates allowed us to hypothesize that an additional resistance, related to fractal geometrical features, contributes to the total resistance against motion. Hypotheses on this resistance are discussed after an analytical investigation of the experiments. The paper describes the methods, and presents experimental and analytical results in both graphical and tabular form, which are commented and interpreted in view of the large number of data points gathered in this experimental campaign.

2. Materials and methods

2.1. Numerical generation of fractal aggregates

Aggregates were generated with a static aggregation algorithm based on Maggi and Winterwerp (2004), where a sequential 3-dimensional face-to-face stochastic assemblage of cubic primary particles from an initial particle with index $i = 1$ was applied until the aggregate was embedded into the minimum cube with dimension $L_c = 32$ primary particles. Aggregate fractal dimension d, porosity ϕ and surface roughness C_k were controlled by the probability for a generic particle i to receive the $n+1$ particle with respect to the addition history index $1 \leqslant i \leqslant n$, where n is the existing number of particles in that aggregate. This probability was defined as

$$Pr[i = i^*] = (Pr[X = X^*])^z \tag{1}$$

where $0 < X \leqslant 1$is a stochastic variable extracted from a uniform probability distribution with a random number generator (i.e., $Pr[X = X^*] = 1/n$) and $z > 0$ is the controlling parameter assigned arbitrarily to generate aggregates with fractal dimensions d skewed toward a specific value. The chosen particle was therefore determined from the integer-rounded index $i^* = \mathrm{I}\{nX^{*z}\}$. Once particle i^* was chosen, the new $n+1$ particle was added to one of the six faces of particle i^* not yet occupied and chosen from a uniform distribution. The probability in Eq. (1) returns low i^* values for $z > 1$ (i.e., aggregates will be relatively dense with high d), and high i^* values for $0 < z < 1$ (i.e., aggregates will be filamentous with clustered masses and low d).

To sample the fractal dimension space with enough values, 6 different increments ranging between $d = 1.9$ ($z = 0.0008$) and $d = 2.71$ ($z = 2.5$) were generated using the above algorithm.

To produce a statistically reliable population, three stochastic replicas of the same aggregate type were generated with unchanged value of z, thus resulting in a total of 18 stochastically generated fractal aggregates grouped 3-by-3 as per similar fractal dimension. Samples of numerically-generated aggregates are depicted in the top row of Fig. 1.

2.2. Lithographic fabrication of fractal aggregates

Numerically-generated aggregates were fabricated by stereolithography (3D printing) using an Objet Eden-250 3D printing apparatus with Fullcure 720 resin (Objet) with $\rho_m = 1.22$ g cm^{-3} specific density. All fabricated aggregates were scaled to give cubic primary particles with size $L_p = 1.56$ mm, thus resulting in specimens of linear size $L = L_c \cdot L_p = 50$ mm. After lithography, aggregates were sunk for 24 h in a sodium hydroxide bath at low concentration to soften unreacted resin used for construction; this was next removed with a gentile water jet. The resulting solid lithography was clean and stable. Note that close pores retained unreacted lithographic resin because not in contact with sodium hydroxide and not accessible for mechanical cleaning. This may have occurred more frequently to aggregates with higher rather than lower fractal dimension, but the overall relative contribution of residual resin to the total aggregate mass and effective density was presumable minor given that the total mass was relatively large for aggregates with high fractal dimension.

Fig. 1 shows a comparison between samples of numerical aggregates and their fabricated twins for each fractal dimension.

2.3. Characteristics of experimental fractal aggregates

Because all particles within numerical aggregates were mapped in space, salient geometrical quantities could be retrieved with relative ease. The fractal dimension was calculated as $d = \log(n)/\log(L/L_p)$ (e.g., Falconer, 1990), where n is the total number of particles, L is the known aggregate linear size, and L_p is the known primary particles size as per above procedures. The aggregate total solid volume was calculated as $V = nV_p$ with $V_p = L_p^3$ the primary particle volume. The volume porosity ϕ was calculated to measure the fraction of voids contained within the equivalent sphere of radius $r_{eq} = (3V/4\pi)^{1/3}$ centered at the centere of mass of the aggregate, thus excluding those outside the equivalent sphere and within the minimum enveloping cube.